

Fig. 4. Unit cell parameters and axial ratios as a function of mole percent PbTiO_3 in BaZrO_3 .

IV. Conclusions

This study has clarified the questions arising from the literature (listed in Section I) as follows:

- (1) The tetragonal-to-cubic transition at 25°C was shown, by determination of the lattice parameters by X-ray diffraction, to occur at a composition of 44 instead of 40⁷ or 46⁸ mole % BaZrO_3 .
- (2) In the compositional range investigated in this system the dielectric, thermal expansion, and reciprocal permittivity data suggested that a phase transition occurs in these materials at a temperature above the Curie temperature. The character of this transition was not investigated.
- (3) Reciprocal permittivity data showed that the transition from a ferroelectric tetragonal phase to a paraelectric cubic phase for the 10, 20, and 30 mole % BaZrO_3 in PbTiO_3 compositions was of first order.
- (4) The addition of BaZrO_3 to PbTiO_3 resulted in a decrease in the Curie temperature of the solid solutions. The dielectric constant showed a maximum of 11,300 at the Curie

temperature for the 20 mole % composition which is larger than the 3400 value reported in the literature.⁶ Other BaZrO_3 concentrations resulted in lower dielectric constant values.

Acknowledgment

The authors acknowledge the fellowship grant from the National Science Foundation, and the partial support from the Office of Naval Research which made this research possible.

References

- ¹ Gen Shirane, Sadao Hoshino, and Kazuo Suzuki, "X-Ray Study of the Phase Transition in Lead Titanate," *Phys. Rev.*, **80**, 1105-1106 (1950).
- ² G. A. Smolenskii, "New Ferroelectric Substances," *Dokl. Akad. Nauk SSSR*, **70**, 405-408 (1950).
- ³ G. A. Smolenskii, "Seignettelectric Properties of Some Perovskite-Type Titanates and Zirconates of Bivalent Metals," *Zh. Tekh. Fiz.*, **20** [2] 137-48 (1950).
- ⁴ H. D. Megaw, "Crystal Structure of Double Oxides of the Perovskite Type," *Proc. Phys. Soc. (London)*, **58** [326, Pt. 2] 133-52 (1946).
- ⁵ T. Ikeda, "Studies on $(\text{Ba,Pb})(\text{Ti,Zr})\text{O}_3$ System," *J. Phys. Soc. Japan*, **14** [2] 168-74 (1959).
- ⁶ S. A. Fedulov, Yu. N. Venetsev, G. S. Zhdanov, and I. S. Rez, "X-Ray and Electrical Investigation of Samples in the System PbTiO_3 ," *Kristallografiya*, **6** [5] 681-85 (1961); *Soviet Phys.-Cryst. (English Transl.)*, **6** [5] 547-50 (1961).
- ⁷ W. R. Bratschun, "Barium Zirconate-Lead Titanate Ferroelectric Ceramics," *J. Am. Ceram. Soc.*, **46** [3] 141-44 (1963).
- ⁸ S. A. Fedulov and Yu. N. Venetsev, "Concerning the Problem of the Transition Region Between Ferroelectric and Paraelectric Phases of $(\text{Pb,Ba})(\text{Ti,Zr})\text{O}_3$ Solid Solutions," *Kristallografiya*, **8** [3] 454-56 (1963); *Soviet Phys.-Cryst. (English Transl.)*, **8** [3] 355-57 (1963).
- ⁹ E. D. Harris, T. Vasilos, and A. P. de Bretteville, Jr., "Sample Holder for Determination of Dielectric Properties of Solids," *Am. Ceram. Soc. Bull.*, **34** [10] 332-33 (1955).
- ¹⁰ Gen Shirane and Sadao Hoshino, "Phase Transition in Lead Titanate," *J. Phys. Soc. Japan*, **6** [4] 265-70 (1951).
- ¹¹ H. E. Swanson, N. Y. Gilfrich, and G. M. Ugrinic, "Standard X-Ray Powder Diffraction Patterns, Vol. 5," *Natl. Bur. Std. (U.S.) Circ.*, No. 539, 75 pp. (1955).

Influence of Water Vapor on Crack Propagation in Soda-Lime Glass

S. M. WIEDERHORN

National Bureau of Standards, Washington, D. C. 20234

Results of a new experimental approach to static fatigue of glass are presented. Using the double-cantilever cleavage technique, it was possible to observe crack motion and to accurately measure crack velocities in glass. The measured crack velocity is a complicated function of stress and of water vapor concentration in the environment. Experimental results are discussed with reference to current theories of static fatigue.

I. Introduction

GLASS is usually regarded as resistant to chemical corrosion and so is used in applications such as enamel coatings for metals and as linings for water heaters and vessels to contain certain chemical reactions. It is therefore surprising that small amounts of water vapor, normally found in the atmos-

phere, react with glass under stress to cause a time-dependent reduction in strength known as static fatigue or delayed failure.

Static fatigue in glass was discovered as early as 1899 by Grenet,¹ who observed that the strength of glass depended on the rate of loading or on the length of time a load was applied. Glass loaded at a rapid rate or forced to support a given load for a short time was relatively strong. In contrast, glass was relatively weak if the loading rate was slow or if the glass was forced to support a given load for a long time. These observations could not at first be explained, but research during the past 30 to 40 years has clarified the

Presented at the Sixty-Eighth Annual Meeting, The American Ceramic Society, May 11, 1966 (Glass Symposium, Paper No. 20-GS-66). Received November 7, 1966.

The writer is physical chemist, Physical Properties Section, National Bureau of Standards.

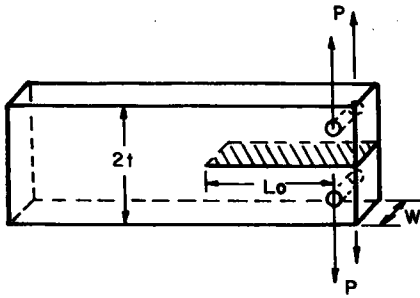


Fig. 1. Specimen configuration.

subject of static fatigue and many of the reasons for this behavior are now known.

The main experimental and theoretical results of static fatigue studies were summarized recently by several authors.²⁻⁴ The dominant belief is that static fatigue results from a stress-dependent chemical reaction between water vapor and the surface of the glass. The rate of reaction depends on the state of stress at the surface, the rate increasing with increasing stress. The stress is greatest at the roots of small cracks in the surface of the glass, and consequently the reaction proceeds at its greatest rate from these roots. Since the reaction products do not have the strength of the unreacted glass, the small cracks gradually lengthen and failure occurs when the cracks are long enough to satisfy the Griffith criterion for fracture.⁵ Thus, two stages of crack growth can be visualized: (1) slow crack motion occurs because of chemical attack at the crack tip, and (2) a catastrophic stage of crack motion initiated when the crack is long enough to satisfy the Griffith criterion. The time to failure in a static fatigue experiment is the time required for the crack to grow from subcritical to critical Griffith size.

Because crack motion is so important in understanding static fatigue, a quantitative investigation of crack motion in soda-lime-silica glass was conducted and the dependence of crack velocity on applied load and environment was determined. It was hoped to obtain some information on the chemical and physical processes occurring at a crack tip during the static fatigue process. This paper continues and extends previous work.^{6,7}

II. Experimental Procedure

Much of the experimental procedure has been described previously,^{6,7} but is reviewed briefly here. The double-cantilever cleavage arrangement used was described by Gilman⁸ (Fig. 1). Specimens were microscope slides of known composition, into which cracks of predetermined length were introduced. A constant force was applied to the ends of the slides and the crack velocity was measured as a function of applied force and environment. Specimen dimensions and crack length were measured before each experimental run, and velocity measurements were obtained using a traveling microscope and a filar eyepiece. Multiple velocity measurements were made on each microscope slide. The higher velocities were usually measured first. A predetermined load was applied to the slide and velocity and crack length were determined. The load was then reduced by a fixed increment and the new velocity and crack length were determined. In this manner, up to 30 data points could be obtained from each microscope slide, depending on the test environment and the velocities measured.

Variations in specimen dimensions and crack length were taken into account by applying a correction to the applied force, as described previously.⁷ The applied force was corrected to the value for a crack length of 3.6 cm and specimen dimensions of $w = 0.15$ cm and $2t = 2.54$ cm. Despite this

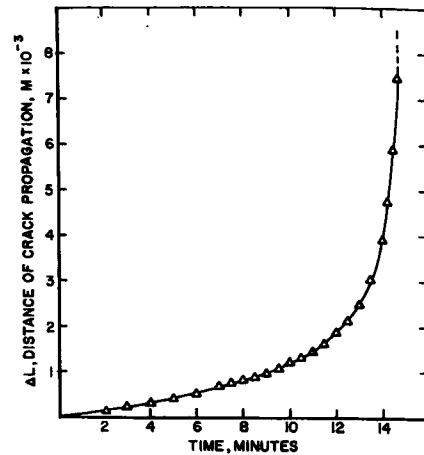


Fig. 2. Crack propagation to failure under constant load, tested in air at 50% rh.

correction, there was still a small dependence of the applied force on crack length, leading to some scatter of the experimental results. Nevertheless, the percent standard deviation in the applied load after correction (2 to 3%) was adequate.

Crack velocities were measured as a function of applied load in gaseous nitrogen at 25°C with relative humidities from 0.0017 to 100% saturation. There was a continuous flow of gas through the test chamber. The slides were annealed at approximately 300°C in a nitrogen gas stream of less than 0.017% rh at 25°C, to remove adsorbed water; they were then tested in the chamber so that they never came in contact with the air during the test period.

III. Results

As predicted previously,² the fracture of glass can be divided into two stages: a growth stage in which the crack motion is relatively slow and a catastrophic stage in which crack motion is rapid and the Griffith criterion is satisfied. The slow stage is shown in Fig. 2 for crack propagation at a constant load in air at 50% rh. The crack velocity gradually increases with time from 8.4×10^{-7} to 1.0×10^{-4} m/sec before the catastrophic stage of crack motion, which could be identified by sudden acceleration of the crack. The shape of the curve is similar to that obtained by Shand from static fatigue data.⁹ More quantitative information on crack motion can be obtained by studying the dependence of crack velocity on force in different environments and at different temperatures.

Figure 3 shows the effect of water vapor on crack motion in glass at room temperature. The data shown represent more than 1000 experimental points, some of which are included in the figure to demonstrate the scatter of the data between runs. The shape of the curves in Fig. 3 can be demonstrated by data from any single run covering a large enough velocity range. One such run may be identified by the open circles in Fig. 3. The plateau in the data is real and is generally exhibited by all runs that cross the plateau region, referred to herein as region II. The sharpness of the plateau is blurred by experimental scatter when all the runs are combined, as is illustrated in the lowest curve of Fig. 3. Portions of the data were fit by straight lines using the method of least squares, minimizing the error along the applied force axis. Crack motion is complex and depends strongly on the amount of moisture in the environment. The curves in Fig. 3, representing 100, 33, 10, 1.0, 0.2, and 0.017% rh are characterized by three distinct regions of crack propagation, which are labeled on the lowest curve. In region I, the crack velocity is exponentially dependent on the applied force $\ln v = \alpha + bP$, and all the curves have similar slopes, b , ranging from 27.6 to

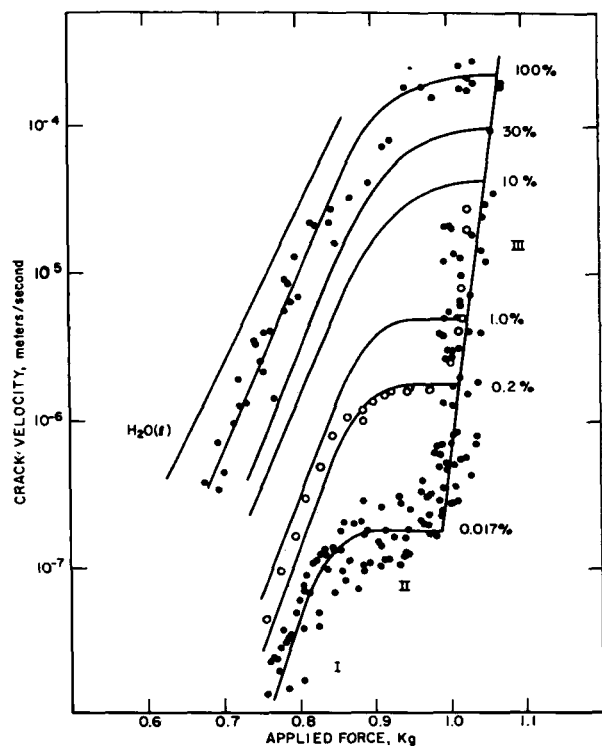


Fig. 3. Dependence of crack velocity on applied force. The percent relative humidity for each set of runs is given on the right-hand side of the diagram. Roman numerals identify the different regions of crack propagation. Region III shows only about half the points used to determine the line. The line, therefore, does not seem to fit the data as well as it would if all data in region III were plotted.

35.6 kg⁻¹ (Table I). The variation of the intercept, α , is due to the systematic dependence of the curves on water vapor concentration, and on the scatter of the slopes, b (Table I). The curves shift to lower velocity and higher force as the relative humidity decreases. The exponential behavior of the curves and the shift with decreasing water concentration can be explained by the Charles-Hillig theory.^{10,11,*} Consequently it is believed that crack propagation in region I is due to corrosive attack of water vapor on the glass at the crack tip.

In region II, the crack velocity is nearly independent of the applied force, and the position of each curve shifts to lower velocities as the water in the environment decreases. This behavior can be explained by assuming that the crack velocity in region II is limited by the rate of water vapor transport to the crack tip. Arguments justifying this assumption, and satisfying the experimental data, are presented in Section IV.

In region III the crack velocity is again exponentially dependent on the applied force; however, the slope of the curve, 92 kg⁻¹, is considerably greater than in region I, 30 kg⁻¹. This change in slope leads to the conclusion that a third crack propagation mechanism occurred. The fact that the curves of regions I and II blend to form a single curve in region III indicates that this new mechanism is independent of water concentration in the environment.

Data for crack propagation in water are included in Fig. 3. The curve falls at higher crack velocity and lower applied force values than the 100% humidity curve; however, the slopes of the two curves are similar (see Table I). Because of this similarity, it is felt that the mechanism of fracture is the same in water as in moist gas. Perhaps the chemical activity of the water at the crack tip differs in the two cases, because corrosion products alter the environment in a liquid by changing its chemical composition.

IV. Discussion of Results

An excellent representation of the velocity data in region I is given by the static fatigue theory of Charles and Hillig^{10,11} (see Appendix I). Their theory assumes that crack motion occurs as a result of a heterogeneous chemical reaction between the glass and the environment at the root of the crack. If their theory is correct, it is necessary, in a general way, to consider the possible successive stages of reaction occurring at the crack tip. Once this has been accomplished, the environmental dependence of crack motion in regions I and II can be explained.

As stated by Glasstone *et al.*¹² "A reaction occurring at a surface may, in general, be separated into five steps, the slowest of which will determine the rate of the overall process. The successive stages are: (1) Transport of gaseous reactants to the surface, (2) adsorption of the gases, (3) reaction on the surface, (4) desorption of the products, and (5) transport of the liberated products from the surface into the bulk gas." Therefore, if crack propagation is due to a heterogeneous chemical reaction, the velocity will be limited by the

* Other theories predict exponential behavior but not a shift of the curves with changing environment.

Table I. Summary of Experimental Data

Percent rh	Slope b (kg ⁻¹)	Intercept α	a (kg-moles/m ² -sec)	v^* (m/sec)	n	Boundary layer thickness, δ (m)
Set (1)						
Water (l)	31.9 ± 3.0	-28.6 ± 2.8				
100	27.8 ± 0.12	-28.2 ± 1.3	6 × 10 ⁻¹²		1	
33	28.5 ± 1.1	-30.1 ± 1.2	3 × 10 ⁻¹²		1	
10	27.6 ± 1.1	-30.9 ± 1.4	4 × 10 ⁻¹²	5.0 × 10 ⁻⁶	1	1.8 × 10 ⁻⁶
1.0	30.0 ± 1.9	-34.4 ± 2.2	1 × 10 ⁻¹⁴	5.0 × 10 ⁻⁶	1/2	3.6 × 10 ⁻⁶
0.2	31.8 ± 2.4	-36.3 ± 2.9	4 × 10 ⁻¹⁵	1.8 × 10 ⁻⁶	1/2	3.6 × 10 ⁻⁶
0.017	34.4 ± 5.3	-39.8 ± 6.5	5 × 10 ⁻¹⁶	1.78 × 10 ⁻⁷	1/2	2.0 × 10 ⁻⁶
Set (2)						
Water (l)	24.5 ± 1.1	-25.2 ± 1.2				
100	27.6 ± 1.9	-29.0 ± 2.1	3 × 10 ⁻¹²	2.3 × 10 ⁻⁴	1	3.9 × 10 ⁻⁶
30	29.3 ± 1.1	-31.6 ± 1.1	7 × 10 ⁻¹³	1 × 10 ⁻⁴	1	2.7 × 10 ⁻⁶
10	32.9 ± 1.6	-35.3 ± 1.8	4 × 10 ⁻¹⁴	4 × 10 ⁻⁵	1	2.3 × 10 ⁻⁶
1	35.6 ± 2.8	-39.1 ± 3.2	1 × 10 ⁻¹⁶	5 × 10 ⁻⁶	1/2	3.6 × 10 ⁻⁶
0.2	31.0 ± 2.5	-36.6 ± 3.1	3 × 10 ⁻¹⁵	1.4 × 10 ⁻⁶	1/2	2.6 × 10 ⁻⁶
0.039	29.2 ± 3.3	-35.6 ± 4.3	2 × 10 ⁻¹⁴	3 × 10 ⁻⁷	1/2	2.4 × 10 ⁻⁶

NOTE: The slope b and intercept α are obtained from a least-squares fit of the data in region I; $\ln v = \alpha + bP$. The constant a is calculated by equating the experimental velocity equation, $v = \exp(\alpha + bP)$, to the theoretical equation (Eq. (9)). Rearranging terms, $a = (n \exp \alpha) / (0.0275 x_0^n)$.

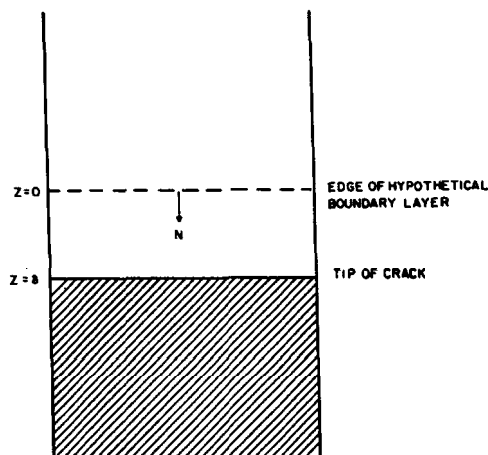


Fig. 4. Cross section of a microscope slide showing crack surface. The cross-hatched area indicates the unbroken portion of the slide.

slowest of these stages. It is reasonable to neglect stages (4) and (5) because the fracture process continually uncovers fresh reaction sites, i.e. new bonds, and as the crack propagates the adsorbed corrosion products are left behind on the walls of the crack and can be expected to have little effect on the rate of reaction. Step (2) may be subdivided into two steps, Van der Waals adsorption and chemisorption. Van der Waals adsorption is physical in nature and, if regarded as an activated process, has an activation energy of the order of 1 kcal/mole, or less.¹³ Because of this low activation energy, Van der Waals adsorption will occur rapidly and consequently will not limit the fracture process. Chemisorption, on the other hand, might limit the fracture process since it is chemical in nature and has a substantial activation energy (5 to 20 kcal/mole, or more).¹³ Therefore the three possible limiting steps for the chemically enhanced fracture process are diffusion, chemisorption, and chemical reaction. The latter two processes involve a chemical reaction with the glass substrate and are expected to depend on the stress at the crack tip, perhaps obeying a reaction law similar to that suggested by Charles and Hillig. Therefore, if fracture were controlled by chemisorption or another chemical reaction at the crack tip, one might expect the crack velocity to be exponentially dependent on the applied force, as observed in region I of Fig. 3. By contrast, if fracture were controlled by the rate of diffusion of water to the crack tip, one would expect the crack velocity to be independent of applied force because diffusion of the gaseous reactants to the surface does not depend on the state of stress at the surface. Since the crack velocity in region II of Fig. 3 is nearly independent of applied force, it is felt that crack propagation in this region is controlled by the rate of water diffusion to the crack tip.

The foregoing ideas can be made quantitative with certain simplifying assumptions which are necessitated by the complex geometry of the crack tip and the possibility of multiple chemical reactions. The treatment used is identical to that given by Bird *et al.*¹⁴ in their discussion of heterogeneous chemical reactions.

Imagine the crack walls to be parallel almost to the crack tip and assume the tip of the crack to be covered by a stagnant boundary layer of nitrogen gas of a thickness δ (Fig. 4). Outside this boundary layer, the mole fraction of water, x_0 , in the gas is assumed to be constant, the water vapor being replenished by bulk flow of nitrogen gas that is sucked in behind the crack as the crack moves. Water vapor is assumed to diffuse through the boundary layer in a direction perpendicular to the crack tip, which permits one-dimensional treat-

ment of the diffusion problem. On diffusing through the boundary layer, the water vapor reacts with the glass at the crack tip according to the rate law, $N = ax^n e^{-bP}$, where a , n , and b are constants; x is the mole fraction of water in the nitrogen next to the crack tip; n is the order of the chemical reaction with respect to water, and N is the number of moles of water per unit area per unit time reacting at the surface. A chemical reaction of this form was chosen because it agrees with that proposed by Hillig and Charles for the static fatigue of glass (see Appendix I). No distinction is made between chemisorption and other possible chemical reactions at the crack tip. The amount of water vapor reacting at the crack tip is equal to the amount diffusing through the boundary layer; therefore, N is also equal to the molar flux of water molecules to the crack tip. N is related to the concentration gradient of water in the boundary layer by the following equation*:

$$N = -c D_{H_2O} \frac{\partial x}{\partial z} + Nx \quad (1)$$

where z is distance from the boundary layer, c is total concentration of water vapor and nitrogen gas in kg-moles/m³, and D_{H_2O} is the diffusivity of water vapor in nitrogen gas. Solving for N and using the fact that for steady state conditions N is constant at any cross section through the boundary layer and that D_{H_2O} and c are constants,

$$\frac{1}{1-x} \frac{dx}{dz} = k_1 \quad (2)$$

Solving Eq. (2) the following equation is obtained for x :

$$-\ln(1-x) = k_1 z + k_2 \quad (3)$$

subject to the following two boundary conditions:

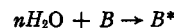
$$\text{I, } x = x_0 \text{ when } z = 0 \quad (4)$$

$$\text{II, } x = \left(\frac{N}{a}\right)^{1/n} \exp(-bP/n) \text{ when } z = \delta \quad (5)$$

Applying the boundary conditions to Eq. (3) the flux of water to the crack tip is

$$N = (cD_{H_2O}/\delta) \ln [1 - (N/a)^{1/n} \exp(-bP/n)] / (1 - x_0) \quad (6)$$

To compare Eq. (6) with the experimental data, the water flux to the crack tip must be related to the crack velocity. An n th order reaction with respect to water suggests that n molecules of water are required to break a single bond, B , of glass,



Therefore, for every molecule of water arriving at the crack, $1/n$ bonds will be broken. Following Charles,² we assume that 3.5×10^{18} bonds are broken for every square meter of crack surface formed and that the bond length is 1.6×10^{-10} m. The number of kg-moles of water required to break 3.5×10^{18} bonds are $3.5n \times 10^{18} / 6.023 \times 10^{26} = 5.82n \times 10^{-9}$ kg-moles. The rate of arrival of water per meter of crack length is $N(1.6 \times 10^{-10})$ kg-moles/sec. After $5.82n \times 10^{-9}$ kg-moles have arrived, the crack will have traveled 1 m. The relation between the flux of atoms to the crack tip and the velocity is

$$v = N(1.6 \times 10^{-10}) / 5.82n \times 10^{-9} = 0.0275N/n$$

This relation is substituted into Eq. (6) to obtain the crack velocity as a function of experimental parameters. The resulting equation for crack velocity is simplified considerably if the argument of the logarithm is expanded into a power series and only first order terms are retained. This is permis-

* The second term on the right of Eq. (1) arises as a result of the stagnant nature of the nitrogen in the boundary layer and represents a flux of water vapor resulting from bulk flow. Derivation of this equation is given in Refs. 14 and 15.

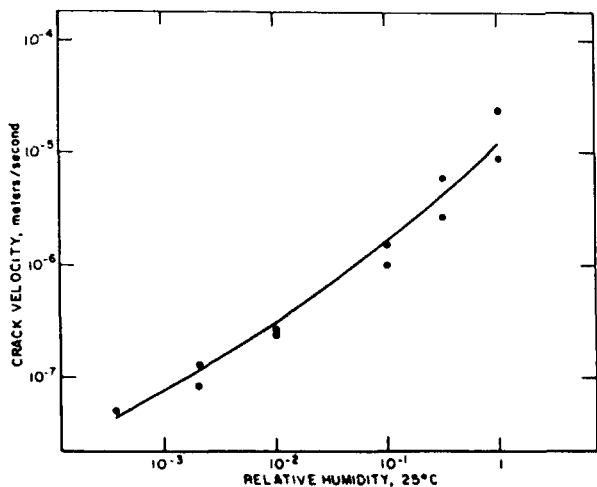


Fig. 5. Dependence of the crack velocity on water vapor concentration in the environment. Data were taken from region I with constant applied force of 0.8 kg. The curve represents the formula $v = 2.11 \times 10^{-6} y^{1/2} + 1.02 \times 10^{-4} y$, where y is relative humidity.

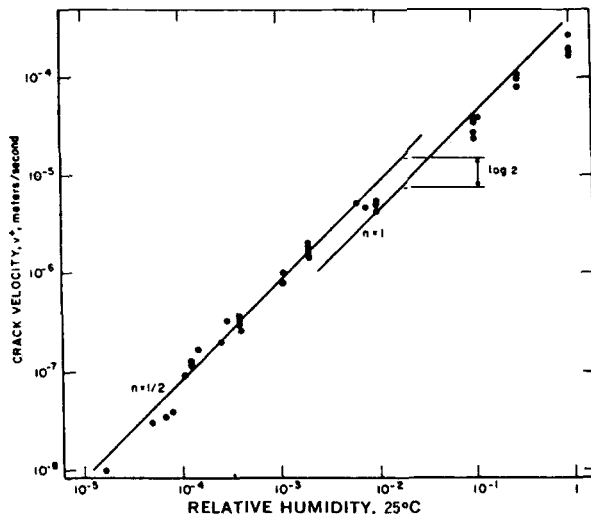


Fig. 6. Dependence of crack velocity v^+ on water vapor concentration in the environment. Data were taken from region II. Lines labeled $n = 1/2$ and $n = 1$ represent the theoretically predicted behavior at low and high concentrations of water vapor, respectively.

sible since x_0 and $(N/a)^{1/n} \exp(-bP/n)$ are small compared to 1. The final equation for the crack velocity is

$$v = v^+ / [1 + (v^+ / x_0 \psi) (nv / 0.0275a)^{1/n} \exp(-bP/n)] \quad (7)$$

where

$$v^+ = 0.0275cD_{H_2O} x_0 / \delta n \quad (8)$$

The limiting forms of Eq. (7) are just those observed in the author's experiments. When the applied force, P , is small, the term of Eq. (7) involving the exponential becomes large with respect to 1 and Eq. (7) reduces to

$$v = (0.0275ax_0^n \exp bP) / n \quad (9)$$

The exponential dependence of velocity on applied force is the behavior observed in region I of the data (Fig. 3). When P is large, the exponential term of Eq. (7) is small compared to 1 and Eq. (7) reduces to $v = v^+$, Eq. (8), and the velocity of crack motion is independent of applied force. This is just the behavior observed in region II of the data. Using experimentally determined values of v^+ , a , b , and n (Table I), Eq. (7) was plotted in Fig. 3 as a set of separate curves, one for each water concentration. Equation (7) fits the data well and accurately describes the shape of the experimental data. In particular, it fits the data in the region of greatest curvature.

Information on the chemical and physical processes occurring during crack motion can be obtained from the dependence of the experimental data on water vapor concentration. Equation (9) predicts that, at constant P , the velocity of crack motion in region I should depend on the partial pressure of water vapor raised to the n th power. Thus, a plot of $\log v$ versus $\log (p_{H_2O} / p^0_{H_2O})$ should give a straight line whose slope is equal to the order of the chemical reaction, n , with respect to water. The data plotted in Fig. 5 do not plot as a straight line. A probable interpretation of this behavior is that more than one reaction is occurring between the water and the glass at the crack tip at a given time. Such behavior might be expected considering the large number of compounds that can form between water and glass.¹⁶ The slope of the data at low relative humidity is approximately $1/2$ whereas at high humidity the slope is 1, suggesting that reactions of order $1/2$ and 1 with respect to water might be occurring at the crack tip. The curve in Fig. 5 was obtained by assuming simultaneous reactions of the order of $1/2$ and 1. The curve

fits the data well; however, the fit cannot be taken as evidence that the suggested orders of reaction are correct without additional experimental confirmation. The fit does, however, demonstrate the type of behavior to be expected from simultaneous reactions.

For crack propagation in region II, Eq. (8) implies that the velocity should be directly proportional to the concentration of water vapor in the environment. Changing the order of the chemical reaction changes the proportionality constant in Eq. (8); therefore a plot of $\ln v$ versus $\ln (p_{H_2O} / p^0_{H_2O})$ should give a set of straight lines of slope 1, each line corresponding to a different order chemical reaction with respect to water. In the present experiment, two straight lines might be expected, one corresponding to a chemical reaction of order $1/2$ and one to a reaction of order 1. The two lines should be displaced from each other along the $\ln v$ axis by $\ln n_1 / n_2 = \ln 2$. The velocity points taken at the lower humidities should lie on the curve for $n = 1/2$ whereas the velocity points at the highest humidities should lie on the curve for $n = 1$. The data from region II are plotted in Fig. 6. The lower humidity points scatter about the straight line for $n = 1/2$; however, the higher humidity points lie below the line for $n = 1$. Therefore the data only partly fit the proposed theory. The discrepancy between theory and experiment probably arises from two sources; (1) the approximation concerning the shape and constant thickness of the diffusional boundary layer at the crack tip, and (2) the uncertain knowledge of the order of the chemical reactions at the crack tip. In contrast to the assumption of a constant boundary layer thickness, the thickness probably depends somewhat on the velocity of crack motion. If the boundary layer were increased in thickness with increasing crack velocity, then the crack velocity in region II, at high velocities, would be less than expected from the simple theory proposed in this paper. Alternatively, the results in Fig. 6 would be explained if the chemical reactions differed from those proposed in this paper. Specifically, the spacing of the straight lines in Fig. 6 would be greater if the ratio of the orders of the chemical reactions, n_1/n_2 , were greater than 2. These discrepancies can be explained only by further experimentation and a more detailed examination of the mechanisms of transport at the crack tip.

No satisfactory theory has been obtained to explain the fracture data in region III. It was thought possible to explain

the data by a thermal fluctuation theory; however, the two theories most easily compared with the data^{3,6,7} are not satisfactory, since they predict that region III should occur at higher applied forces than they actually do. Another possibility is that motion in region III is controlled by dynamic considerations in the manner described by Berry¹⁷ and that the onset of motion is determined by the Griffith criterion for fracture. If this were the case it could be shown, using Berry's¹⁷ dynamic equations, that crack acceleration would be so rapid that the microscope slides would appear to fracture instantaneously. Since crack motion in region III was easily observed, it is obvious that region III does not correspond to dynamically controlled crack motion. A final possibility is that crack motion in region III is caused by a physical or chemical process internal to the glass, such as diffusion of an ionic species or water to the crack tip where reaction and bond breakage can occur.

V. Summary

The double-cantilever cleavage technique was used to study the effect of water vapor on crack propagation in soda-lime glass. The crack motion was complex, depending strongly on environment. Three regions of motion were identified. Crack motion in region I was limited by the rate of reaction of water with the glass at the crack tip. In region II the crack motion was limited by the rate of transport of water vapor to the crack tip. Based on the static fatigue theory of Charles and Hillig,^{10,11} a combined rate equation was developed to account for the experimental data in regions I and II. The equation successfully accounts for the shape of the experimental data in regions I and II, but only partly accounts for the dependence of crack velocity on water vapor concentration. The disagreement between theory and experiment is believed to be due to uncertain knowledge of the chemical reactions occurring at the crack tip and the simplifying assumptions concerning the mass transport processes at the crack tip.

A third region of crack motion was studied in which crack motion seemed to be independent of the amount of water vapor in the environment; however, no satisfactory explanation has been found for crack propagation in region III.

APPENDIX I

The theory of static fatigue that best satisfies available experimental data was developed by Charles and Hillig,^{10,11} who assumed that the corrosion reaction at the crack tip was an interfacially controlled activated process with a stress-dependent activation energy. They developed the following equation for the velocity of a moving crack under the influence of a corrosive environment and a crack tip stress σ ,

$$v = v_0 \exp - [E^*(0) - V^*\sigma + c\sigma^2 + \Gamma V_m/2\rho]/RT \quad (10)$$

$E^*(0)$ is the activation energy for surface corrosion at a stress-free surface and V^* is the activation volume for the process. The term $c\sigma^2$ represents the combined effect of the disappearance of strain energy due to corrosion and a second order term in the expansion of the activation energy. The term $\Gamma V_m/2\rho$ represents the effect of curvature of the reaction surface; Γ is the surface free energy of the glass corrosion product interface; V_m is the molar volume of the glass, and ρ is the radius of curvature of the crack tip. Experiments^{3,7} on the effect of temperature on crack velocity have confirmed the validity of Eq. (10). The σ^2 term and the surface energy term are small compared to the other terms in the exponential of Eq. (10) and can be neglected to a good approximation. If it is also assumed that the crack tip stress, σ , is proportional to the applied force P , the following crack velocity equation is obtained:

$$v = v_0 \exp - [E^*(0) - \beta P]/RT \quad (11)$$

Eq. (11) describes the experimental results in region I.

Since $E^*(0)$ is a function of environment, Eq. (10) or (11) can be naturally extended to account for changing moisture content

in the environment. Based on 1 mole of reacting glass bonds, the equation for chemical reaction at a free surface is



where n is the number of water molecules reacting with a bond, B , to form an activated complex, B^* . $E^*(0)$ can be expressed as the difference in chemical potential between the reactants and product of the corrosion reaction

$$E^*(0) = \mu_{B^*} - \mu_B - n\mu_{\text{H}_2\text{O}} \quad (13)$$

where μ_{B^*} is the chemical potential of the activated state, μ_B is the chemical potential of a bond, and $\mu_{\text{H}_2\text{O}}$ is the chemical potential of water. Assuming water behaves as a perfect gas,

$$\mu_{\text{H}_2\text{O}} = RT[\Phi(T) + \ln p_{\text{H}_2\text{O}}] \quad (14)$$

where $\Phi(T)$ is some function of temperature and $p_{\text{H}_2\text{O}}$ is the partial pressure of water. Substituting Eqs. (13) and (14) into Eq. (11), the crack velocity is

$$v = v_0 (p_{\text{H}_2\text{O}})^n \exp - [\mu_{B^*} - \mu_B - nRT\Phi(T) - \beta P]/RT \quad (15)$$

At a constant temperature, assuming that μ_{B^*} and μ_B are independent of environment, and for a single chemical reaction, constant n , the following equation is obtained:

$$v = cx^n \exp bP \quad (16)$$

where x is the mole fraction of water vapor at the crack tip. If it is now assumed that the crack velocity is proportional to the rate of chemical reaction at the crack tip, the following equation is obtained:

$$N = ax^n \exp bP \quad (17)$$

where N is the number of moles of water per unit area per unit time reacting at the crack tip. Equation (17) is identical to the one used in the derivation of the combined reaction rate equation.

APPENDIX II

In the previous sections, factors such as corrosion product expansion, surface diffusion, and liquid phase condensation at the crack tip have been ignored. Since these factors might affect the stress corrosion process, brief comments will be made on these effects.

Occlusion of the crack tip by corrosion products would change the mechanism of crack propagation, for then the water vapor would have to diffuse through a layer of corrosion product to reach the crack tip. The mathematical treatment of this situation would be identical to the one described in the foregoing, with minor changes. The corrosion layer thickness would be substituted for the gas diffusion layer thickness and the diffusion coefficient for water in the corrosion layer would be substituted for the diffusion coefficient of water vapor in gaseous nitrogen. Since the equations obtained by this substitution would be identical to those obtained in the foregoing, either crack growth mechanism would describe the results satisfactorily. The same conclusion may be drawn concerning surface diffusion of water to the crack tip, provided the surface diffusion coefficient and the surface diffusion thickness are substituted for the corresponding gas quantities. Thus the experiments may be described equally well by assuming gas or surface diffusion to the crack tip, or by assuming the occurrence of a corrosion layer at the crack tip. Consequently, it is not readily apparent which process is actually occurring during our experiments.

It is possible that the crack tip contains a pocket of water rather than being filled with gas as assumed in the foregoing derivation. If water were at the crack tip the gas diffusion mechanism proposed to explain the experimental results would be invalidated. Therefore it is necessary to discuss this possibility.

The collection of water at the crack tip is governed in part by thermodynamic considerations and depends on the temperature, water vapor pressure, and equilibrium radius of curvature of the water meniscus at the crack tip. A crack tip con-

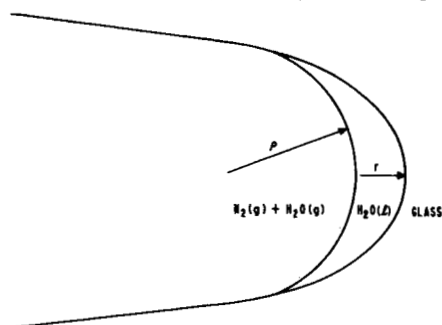


Fig. 7. Schematic diagram of a water pocket at a crack tip.

taining a water pocket has been idealized in Fig. 7, in which r is the radius of curvature of the crack tip and ρ is the radius of curvature of the water meniscus. The condensation of water is governed by the Kelvin equation¹⁸

$$\ln(p_0/p) = -2\Gamma V/\rho RT$$

where p_0 is the water vapor pressure over a flat surface and p is the water vapor pressure over water of curvature ρ ; Γ is the surface tension of water, 0.072 joules/m²; V is the molar volume of water, 0.018 m³/kg-mole; R is the gas constant, and T is the absolute temperature. Water transport from the gas to the water pocket will occur if the water vapor pressure of the gas environment, p_0 , is greater than the water vapor pressure of the water meniscus, p , at the crack tip, $p_0 > p$. Conversely, water transport will be in the reverse direction if $p > p_0$. When $p_0 = p$, the system is in equilibrium. For a system not initially in equilibrium, the water transport will change the size of the water pocket which in turn changes the meniscus radius, ρ , in such a manner that p approaches p_0 . At equilibrium, $p = p_0$, the meniscus radius will have a characteristic value, ρ_0 , which can be calculated from the Kelvin equation by setting $p = p_0$ and $\rho = \rho_0$. A comparison between p_0 and ρ_0 is presented in Table II for various percentages of relative humidity. An interesting aspect of Table II is the rapid decrease in meniscus radius, ρ_0 , for gases containing relatively high concentrations of water vapor. From simple optical considerations it can be shown that a crack will become visible in reflected radiation when the spacing between the crack surfaces is of the order of the wavelength of light, 10^{-7} m, which means that water will not be observed at the crack tip unless the atmosphere is nearly saturated, $p_0/p_0 \sim 0.99$. Another aspect of Table II is the extremely small meniscus radius for relative humidities of less than 30%. In fact it is not very probable that a condensed phase with a meniscus radius of less than 10^{-9} m can exist at a crack tip because of the finite volume of the water molecule in the liquid state, which is 3×10^{-29} m.³ The cube root of this value gives an estimation of the spacing between water molecules in the liquid state, 3.1×10^{-10} m, which means that for ρ_0 of the order of 10^{-9} m only a few water molecules could be packed into the crescent representing the water pocket in Fig. 7. This could hardly constitute a liquid water phase. Thus, it may be concluded that liquid water does not exist at the crack tip for vapor concentrations of less than about 35% rh. Near saturation, however, liquid water may exist at the crack tip.

In the foregoing discussion the liquid at the crack tip was assumed to be pure water when in fact if there were a liquid at the crack tip it would be an aqueous solution containing corrosion products. The main effect of the solute in the liquid phase would be to reduce the equilibrium water vapor pressure of the solution below that of water. From an extrapolation of the vapor pressure data in the literature,^{19,20} a knowledge of the Na₂O-SiO₂-H₂O phase diagram,²¹⁻²³ and assuming the liquid phase to be a saturated solution containing Na₂O and SiO₂, it can be shown that the maximum possible reduction in vapor pressure occurs for a solution of Na₂O·2SiO₂ and is about 6 mm

Table II. Dependence of Meniscus Radius on Relative Humidity

Percent rh in atm (100(p ₀ /p ₀))	Meniscus radius, ρ ₀ (m)	
	Pure water	Na ₂ Si ₂ O ₅ solution (saturated)
100	∞	
99	-1.0 × 10 ⁻⁷	
90	-1.0 × 10 ⁻⁸	
75	-3.7 × 10 ⁻⁹	
30	-8.8 × 10 ⁻¹⁰	∞
10	-3.4 × 10 ⁻¹⁰	-1.2 × 10 ⁻⁹
1	-2.3 × 10 ⁻¹⁰	-5.2 × 10 ⁻¹⁰
0.2	-1.7 × 10 ⁻¹⁰	-2.4 × 10 ⁻¹⁰
0.0017	-1.2 × 10 ⁻¹⁰	-1.8 × 10 ⁻¹⁰
		-1.3 × 10 ⁻¹⁰

Hg, which leads to a value of p_0 of 18 mm Hg rather than 24 mm Hg for pure water. The solution meniscus radii calculated for a saturated solution of Na₂O·2SiO₂ are given in Table II. The small values of the meniscus radii preclude the existence of solution at the crack tip in nitrogen gas of less than 30% rh. At humidities of approximately 75% and greater, an aqueous solution probably will exist at the crack tip.*

The existence of a liquid phase at the crack tip can be influenced by dynamic as well as by static considerations. In a real situation of a crack moving under the influence of a moist environment, water continually reacts with the crack tip and corrosion products are continuously entering the liquid pocket. For a steady state condition, the existence of a solution pocket will depend on the relative rates of water and corrosion product addition to the liquid phase. The liquid pocket may dry up if the water transport to the liquid phase is not great enough to supply water for the bond-breaking chemical reaction plus a surplus to maintain the solution. Thus the crack tip may be dry even though the equilibrium meniscus should be large enough for a solution to exist at the crack tip.

The high viscosity of sodium silicate solution, 10² to 10⁴ cp for high concentrations,²⁴ also influences the possible existence of a liquid phase at the crack tip. As the crack moves, the liquid pocket must be fluid enough to keep up with the crack tip. If not, it will tend to stick to the crack walls and be left behind. Thus any concentrated sodium silicate solution initially at the crack tip will tend to disappear as the crack moves.

In summary, the only environment used in our tests in which there is a possibility of a liquid at the crack tip is a 100% rh environment, and even here, the crack tip may be dry for a moving crack due to the viscosity of the sodium silicate solutions and the greater rate of water transport required to maintain a solution over that required for the bond-breaking chemical reaction. In view of the consistent variation of the experimental results with moisture content of the environment, it is believed that the crack tips were dry during the experiments.

Acknowledgment

The author expresses gratitude to J. B. Wachtman, Jr., W. K. Haller, and W. Capps for critical review of this manuscript and for helpful suggestions.

References

- Louis Grenet, "Mechanical Strength of Glass," *Bull. Soc. Enc. Industr. Nat. Paris*, (Ser. 5), 4, 838-48 (1899).
- R. J. Charles; pp. 1-38 in *Progress in Ceramic Science*, Vol. 1. Edited by J. E. Burke. Pergamon Press, New York, 1961.
- W. B. Hillig; pp. 152-94 in *Modern Aspects of the Vitreous State*, Vol. 2. Edited by J. D. Mackenzie. Butterworth, Inc., Washington, D. C., 1962.
- C. J. Phillips, "Strength and Weakness of Brittle Ma-

* If one included the effect of solute on Γ and V , an increase of about 40% in the value of ρ_0 for the solution meniscus radius might be expected. This increases the possibility of water at the crack tip in the 30% humidity environment, but leaves the conclusions unchanged for drier environments.

terials," *Am. Scientist*, 53 [1] 20-51 (1965).

⁶ (a) A. A. Griffith, "Phenomena of Rupture and Flow in Solids," *Phil. Trans. Roy. Soc. (London)*, 221A, 163-98 (1920).

(b) A. A. Griffith, "Theory of Rupture," *Proc. First Intern. Congr. Appl. Mechanics, Delft*, pp. 55-63 (1924).

⁶ S. M. Wiederhorn; pp. 503-28 in *Materials Science Research, Vol. 3*. Edited by W. W. Kriegel and Hayne Palmour III. Plenum Press, New York, 1966.

⁷ S. M. Wiederhorn; pp. 293-317 in *Environment-Sensitive Mechanical Behavior of Materials*. Edited by A. R. C. Westwood and N. S. Stoloff. Gordon and Breach, New York, 1966.

⁸ J. J. Gilman, "Direct Measurements of Surface Energies of Crystals," *J. Appl. Phys.*, 31 [12] 2208-18 (1960).

⁹ E. B. Shand, "Fracture Velocity and Fracture Energy of Glass in the Fatigue Range," *J. Am. Ceram. Soc.*, 44 [1] 21-26 (1961).

¹⁰ R. J. Charles and W. B. Hillig; pp. 511-27 in *Symposium on Mechanical Strength of Glass and Ways of Improving It*. Florence, Italy, September 25-29, 1961. Union Scientifique Continentale du Verre, Charleroi, Belgium, 1962.

¹¹ W. B. Hillig and R. J. Charles, pp. 682-705 in *High-Strength Materials*. Edited by V. F. Zackey. John Wiley & Sons Inc., New York, 1965.

¹² Samuel Glasstone, K. J. Laidler, and Henry Eyring, *Theory of Rate Processes*, p. 369. McGraw-Hill Book Co., New York, 1941.

¹³ Samuel Glasstone, *Textbook of Physical Chemistry*, 2d ed.; p. 1201. D. Van Nostrand Co., Inc., New York, 1946.

¹⁴ R. B. Bird, W. E. Stewart, and E. N. Lightfoot, *Transport Phenomena*; pp. 519, 529. John Wiley & Sons, Inc., New York, 1960.

¹⁵ J. M. Coulson and J. F. Richardson, *Chemical Engineering*, Vol. I, p. 236. McGraw-Hill Book Co., New York, 1955.

¹⁶ *Handbook of Chemistry and Physics*, 47th ed.; p. 646. Chemical Rubber Publishing Co., Cleveland, Ohio, 1966.

¹⁷ J. P. Berry, "Some Kinetic Considerations of the Griffith Criterion for Fracture: I," *J. Mech. Phys. Solids*, 8 [3] 194-206 (1960).

¹⁸ W. Thomson (Lord Kelvin), "Equilibrium Vapour at a Curved Surface of Liquid," *Phil. Mag.*, 42, 448-52 (1871).

¹⁹ A. N. C. Bennett, "Some Vapor Pressures and Activities of Aqueous Solution of Sodium Silicates," *J. Phys. Chem.*, 31, 890-96 (1927).

²⁰ R. W. Harman, "Aqueous Solutions of Sodium Silicates: V," *ibid.*, pp. 355-73.

²¹ C. L. Baker and L. R. Jue, "System $\text{Na}_2\text{O}-\text{SiO}_2-\text{H}_2\text{O}$: Isotherms at 10° and 31°C," *J. Phys. & Colloid Chem.*, 54, 299-304 (1950).

²² J. H. Wills, "A Review of the System $\text{Na}_2\text{O}-\text{SiO}_2-\text{H}_2\text{O}$," *ibid.*, pp. 304-10.

²³ C. L. Baker, L. R. Jue, and J. H. Wills, "System $\text{Na}_2\text{O}-\text{SiO}_2-\text{H}_2\text{O}$ at 50, 70, and 90°," *J. Am. Chem. Soc.*, 72, 5369-82 (1950).

²⁴ Stericker; Ph.D. Dissertation, University of Pittsburgh, Pennsylvania, 1922. Values reported in *International Critical Tables*, Vol. V, p. 16. McGraw-Hill Book Co., New York, 1926-1933.

Transformation of Quartz to Tridymite in the Presence of Binary Silicate Liquids

GERALD I. MADDEN* and LAWRENCE H. VAN VLACK

Department of Chemical and Metallurgical Engineering, The University of Michigan, Ann Arbor, Michigan 48104

The isothermal transformation rates for quartz to tridymite were studied in the presence of binary silicate liquids between the eutectic temperature and 1470°C. Oxide pairs included $\text{Na}_2\text{O}-\text{SiO}_2$, $\text{PbO}-\text{SiO}_2$, $\text{FeO}-\text{SiO}_2$, and $\text{Cu}_2\text{O}-\text{SiO}_2$. Micrographic and X-ray analytical procedures were used. Transformation was most rapid at intermediate temperatures, thus providing typical TTT curves. The rates increased as the liquid contents of the binary pairs were increased. Transformation was more rapid for the pairs which had higher SiO_2 contents in their equilibrated liquids. Transformation proceeded as a solution-reprecipitation reaction. Initially, metastable cristobalite precipitated more rapidly than the tridymite; however, it redissolved and eventually disappeared, leaving only tridymite as the solid phase. An empirical equation was adapted to the transformation.

I. Introduction and Previous Work

THE reconstructive silica transformations, in contrast to the low-to-high displacive transformations, have been qualitatively described as sluggish.¹ This investigation was undertaken to determine the effect of temperature and composition on the rate of the reconstructive transformation of quartz to tridymite in the presence of a liquid phase containing SiO_2 and another oxide. The systems studied were: $\text{Na}_2\text{O}-\text{SiO}_2$, $\text{PbO}-\text{SiO}_2$, $\text{FeO}-\text{SiO}_2$, and $\text{Cu}_2\text{O}-\text{SiO}_2$.

In a study of the influence of iron oxide on the rate of quartz inversion in lime and lime-clay bonded silica brick,

Hugill and Rees² found that the transformation of quartz to tridymite was promoted by the presence of iron oxide, but obtained no quantitative information to describe the reaction rates. In addition, they observed that the presence of tridymite increased the cross-breaking strength, the modulus of rupture, and the crushing strength of brick.

Grimshaw *et al.*³ studied the kinetics of quartz transformation in the presence of various additives (Fe_2O_3 , CaO , MgO , Al_2O_3 , and TiO_2). The important factors in the transformation process were the presence of liquid, subdivision of the solid catalysts, and the type of oxide added.

A study of the effects of the addition of alkali oxides to quartz on the formation of tridymite was reported by De Keyser and Cypres,⁴ who found that tridymite forms more rapidly in the presence of Na_2O and K_2O than in the presence of Li_2O at the same molar concentrations and temperatures. The

Presented at the Sixty-Eighth Annual Meeting, The American Ceramic Society, Washington, D. C., May 10, 1966 (Basic Science Division, No. 35-B-66). Received January 20, 1966; revised copy received January 30, 1967.

This work forms part of a thesis submitted by G. I. Madden in partial fulfillment of the requirements for the degree of Doctor of Philosophy in metallurgical engineering, Horace Rackham School of Graduate Studies, The University of Michigan, 1965.

This work was supported by the United States Office of Naval Research under Contract No. Nonr 1224(47).

At the time this work was done the writers were, respectively, graduate student, and professor and associate chairman, Department of Chemical and Metallurgical Engineering, The University of Michigan.

* Now research scientist, Paul D. Merica Research Laboratory, The International Nickel Company, Incorporated, Sterling Forest, Suffern, New York 10901.